연세대학교
YONSEI UNIVERSITY

Effects of Bismuth Breast Shielding on Dual-Energy Computed Tomography: An Experimental Phantom Study

Hyunsik Jang

Department of Medicine

The graduate School, Yonsei University

연세대학교
YONSEI UNIVERSITY

Effects of Bismuth Breast Shielding on Dual-Energy Computed Tomography: An Experimental Phantom Study

Directed by Professor Hye-Jeong Lee

The Master's Thesis

submitted to the Department of Medicine

The Graduate School of Yonsei University

in partial fulfillment of the requirements for the degree

of Master of Medical Science

Hyunsik Jang

June 2016

This certifies that the Master's Thesis of

Hyunsik Jang is approved.

Thesis Supervisor : Hye-Jeong Lee

Thesis Committee Member#1 : Jin Hur

Thesis Committee Member#2 : Inkyung Jung

The Graduate School

Yonsei University

June 2016

ACKNOWLEDGEMENTS

I would like to express the deepest appreciation to my supervisor professor Hye-Jeong Lee for supporting my efforts with total commitment and facilitating every step of the process. She continually and convincingly conveyed a spirit of adventure in regard to research and scholarship, and an excitement in regard to teaching. Without her guidance and persistent help, this dissertation would not have been possible.

I am also indebted to my committee members, Professor Jun Hur and Inkyung Jung, for their help for pertinent advice to assure the superior quality of this paper. Additionally, I am grateful to Kyung-Hwa Han for her help with the statistical support.

<TABLE OF CONTENTS>

LIST OF FIGURES

LIST OF TABLES

ABSTRACT

Effects of Bismuth Breast Shielding on Dual-Energy Computed Tomography: An Experimental Phantom Study

Hyunsik Jang

Department of Medicine

The Graduate School, Yonsei University

(Directed by Professor Hye-Jeong Lee)

PURPOSE: The purpose of this study is to evaluate the effects of bismuth breast shielding on iodine quantification and radiation exposure in dual-energy computed tomography (DECT).

MATERIALS AND METHODS: Ethics approval was not required for this phantom study. Small balloons were filled with mixtures of water and iodinated contrast (0.2%, 0.6% and 1.0%) to mimic lung nodules. The balloons were located at the anterior and posterior aspects of both lungs in the phantom. DECT was performed with and without breast shielding. Afterwards, iodine overlay attenuation values were measured for each nodule on the iodine maps. Absorbed radiation doses were also measured at the breast. A total of 12 pairs of data from DECT performed with and without breast shielding were obtained for iodine overlay attenuation values of the nodules in each location for each concentration and for radiation doses. Results were compared using the Wilcoxon signed-rank test.

RESULTS: Iodine overlay attenuation values for the 0.2%, 0.6% and 1.0% nodules significantly decreased after breast shielding at the anterior location (P = 0.002 for all). Values significantly decreased after breast shielding at the posterior location for the 0.2%, 0.6% and 1.0% nodules as well (P = 0.002 for all). Absorbed radiation doses to the breast significantly decreased after breast shielding with a reduction rate of 14.8% (P = 0.005)

CONCLUSION: Although the bismuth breast shield can decrease radiation exposure to the breast during DECT, it can significantly affect the results of iodine quantification.

Key words: bismuth breast shield, absorbed radiation dose, dual-energy CT, iodine quantification

Effects of Bismuth Breast Shielding on Dual-Energy Computed Tomography: An Experimental Phantom Study

Hyunsik Jang

Department of Medicine

The Graduate School, Yonsei University

(Directed by Professor Hye-Jeong Lee)

I. INTRODUCTION

With dual-energy computed tomography (DECT), materials can differentiated through energy-dependent photoelectric absorption and variable K-edges with the simultaneous usage of low and high x-ray energies [1-4]. Although the concept of DECT was initially described in the 1970's [5-7], it has recently developed at a fast pace with advanced techniques being introduced such as dual x-ray sources, rapid tube potential switching or multilayer detectors. DECT has been increasingly applied to clinical practice, especially to detect and quantify iodine which is now well established as the standard contrast material for CT [3]. Although some specialists have conflicting opinions, several literatures have reported that DECT could result in higher radiation exposure compared to conventional single energy CT [8,9].

With recent significant increase of diagnostic CT examination, public health concerns about the exposure radiation, which can be a potential risk of malignancy [10-12]. Among the many organs in the human body, the breast is one of the most susceptible to ionizing radiation especially during adolescence [12]. Additionally, the breast is directly irradiated during thoracic and abdominal CT scans even when it is not the organ of interest. For these reasons, an in-plane bismuth breast shield has been used to selectively reduce radiation exposure to the breast and the reduction rate of radiation exposure has been reported to range from 29 to 59% with breast shielding [13-19]. Based on these findings, we can expect the bismuth breast shield to reduce radiation exposure to the breast during DECT as well. However, incorporating the bismuth breast shield also entails some drawbacks. The highly attenuating shield increases image noise and is the cause of beam hardening and streak artifacts [13]. Moreover, a few studies reported the attenuation shift effect on CT [20]. Hence, we thought that image noise, artifacts and attenuation distortion from the bismuth breast shield could potentially affect material differentiation and quantification on DECT. However, to our best knowledge, there has been little study on the effects of bismuth breast shielding on DECT despite increased use of DECT for the thorax, which covers the area under the shield [1,4,21]. Therefore, we evaluated the effects of bismuth breast shielding on DECT focusing on iodine-based material differentiation and quantification in addition to image noise and radiation dose through a phantom study.

II. MATERIALS AND METHODS

1. Phantom and bismuth shielding

Ethics approval was not required for this phantom study. An adult anthropomorphic chest phantom (N1 LUNGMAN; Kyoto Kagaku Co., Japan) was used because of its accurate chest anatomy structure. Small balloons approximately 10 mm in diameter were used to mimic lung nodules. These balloons were filled with mixtures of water and iopamidol-based contrast medium (370mg/ml of iodine, Iopamiro370, Bracco, Milano, Italy) of different concentrations. We preliminarily made balloons with 1.0%, 3.0% and 5.0% iodine to determine the proper iodine concentration for this study and the Hounsfield Unit of each balloons were about 110HU, 350HU and 550HU, respectively. Because the HU of non-calcified lung nodule is mostly less than 200 HU in clinical filed, we decided to make balloons with 0.2%, 0.6% and 1.0% concentration of Iopamidol (Figure 1). Twenty four balloons were made for each iodine contrast concentration.

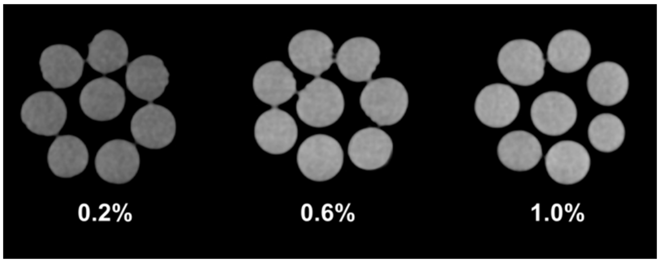

Figure 1. CT images of small balloons approximately 10 mm in diameter mimicking lung nodules. These balloons were filled with mixtures of water and iopamidol-based contrast medium of three different concentrations (0.2%, 0.6% and 1.0%).

A commercially available bismuth breast shield (AttenuRad; AttenuTech, Lutz, FL) was used in this study. The shield consisted of 1-mm thick bismuth-impregnated synthetic rubber and an additionally attached 10-mm thick foam offset, which provided a small gap between the shield and the anterior chest wall. The shield was located over the anterior chest wall with phantom-contouring.

2. CT scan protocol

All CT scans were performed with a second-generation dual-source DECT (SOMATOM Definition Flash; Siemens Healthcare, Erlangen, Germany). Four balloons with the same concentration were located at the anterior and posterior aspect of both lungs in the phantom. One set of CT scans consisted of images obtained without breast shielding and images obtained with breast shielding after the localizer scan. CT scans were performed with the dual-energy technique with the following scan parameters. Tube voltages and currents were 100 kV and 89 reference mAs for the A tube and 140 kV and 76 reference mAs for the B tube. Detector collimation was 64 x 0.6 mm, matrix 512 x 512, pitch 0.5, and gantry rotation time 280 msec. After one set of CT scans was acquired, the 4 balloons were removed. Another 4 balloons of the same concentration were then positioned at identical locations and CT scanning was repeated with the same protocol. A total of 6 sets of DECT scans were obtained, and finally, 12 pairs of CT data acquired with and without breast shielding for each concentration were obtained from the anterior and posterior locations, respectively. From the raw data, images were automatically reconstructed from each tube using a 1-mm slice thickness, a 1-mm increment interval, and a medium-smooth convolution kernel (D30f). In addition, weighted-average 120-kV images were reconstructed, which were fused with 60% information from the 100 kV images and 40% from the 140 kV images.

3. Image analysis

All images were transferred to a commercially available workstation (Syngo MMWP VE23A, Siemens Medical Solutions, Forchheim, Germany). Iodine overlay images for the nodules were made to extract iodine using a prototype of the “Lung nodule” application class of the workstation with adjusted material parameters as follows: -103 Hounsfield unit (HU) for fat at 100 kV; -87 HU for fat at 140 kV; 52 HU for soft tissue at 100 kV; 51 HU for soft tissue at 140 kV; relative contrast material enhancement, 2.24; minimum value, -200 HU; maximum value, 3071 HU; 2 for range, which controls the size of the spherical three-dimensional filter kernel in units of the voxel size; and -100 HU for the contrast media cutoff value.

A single observer (H.J.L) with 9 years of experience in chest CT drew circular regions of interest (ROIs) at the mid-level of each nodule on the iodine overlay images. ROIs were drawn manually for each nodule to avoid edges that were prone to partial volume averaging. From each ROI, the iodine overlay attenuation value, defined by the attenuation difference caused by iodine through material decomposition, was recorded (Figure 2). A total of 12 pairs for the iodine overlay attenuation values with and without breast shielding were obtained for each concentration from the anterior and posterior locations, respectively. In addition, the observer drew ROIs at identical locations on the corresponding 100-kV and 140-kV CT images for each nodule to obtain the CT attenuation value of each kV.

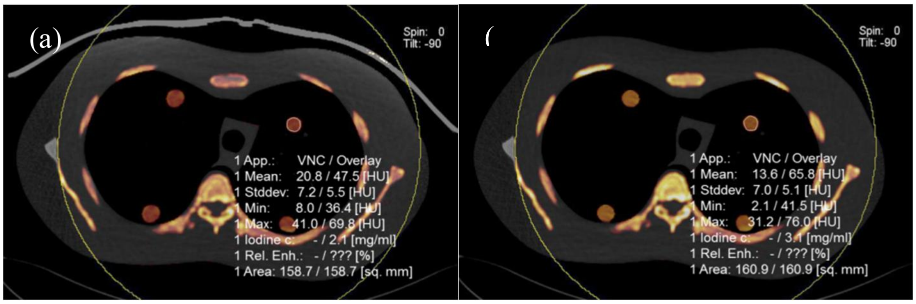

Figure 2. Iodine color-coded maps from the dual-energy CT scans for nodules with 0.6% iodine concentration. Four balloons with the same iodine concentration were located at the anterior and posterior aspects of both lungs. On the iodine map obtained without the bismuth breast shield (a), iodine overlay attenuation values of the nodules are presented as yellow-orange (iodine overlay attenuation value, 65.8 HU). However, values are significantly decreased to dark orange after bismuth breast shielding (iodine overlay attenuation value, 47.5 HU) (b).

Objective image quality was assessed for image noise by measuring the standard deviations of the CT attenuation values of the lung on weighted-average 120-kV CT images, which are usually used for visual examination as conventional CT images. The observer placed the circular ROIs in the anterior and posterior locations 1 cm from the chest wall of the right and left lungs at the carina level of the phantom. ROIs were kept constant in location and size between the CT images with and without breast shielding. Thirty six pairs of standard deviations were obtained with and without breast shielding from the anterior and posterior locations respectively.

4. Measurement of absorbed radiation dose

The optically stimulated luminescence dosimeter nanoDOT™ and MicroStar reader® (Landauer, Inc., Glenwood, IL, USA) were used to measure and analyze radiation exposure. Four dosimeters were placed at the right and left anterior chest wall and the center of the right and left lung, respectively to simulate and measure the radiation absorbed by the breast and lung. After each CT scan, dosimeters were removed from the phantom for read-out and new dosimeters were placed in the phantom. A total of 6 sets of DECT scans with and without breast shielding were performed with the same protocol as above and radiation doses for the 12 pairs, with and without breast shielding, were obtained for the breast and lung, respectively.

5. Statistical analysis

Statistical analysis was performed with commercially available statistics software (SPSS, version 23.0, IBM Software). Quantitative variables were expressed as mean ± standard deviation and normality was tested by the Komogorov-Smirnov test. Iodine overlay attenuation values and CT attenuation values for each kV were compared for CT scans performed with and without breast shielding using the Wilcoxon signed-rank test for each location. Values for location, anterior and posterior, were also compared. Radiation doses for the breast and lung, and image noise for the anterior and posterior locations were also compared between CT scans performed with and without breast shielding using the Wilcoxon signed-rank test. $P < 0.05$ indicated a significant difference.

III. RESULTS

1. Comparison of iodine overlay attenuation values

Measured iodine overlay attenuation values are shown in Figure 3.

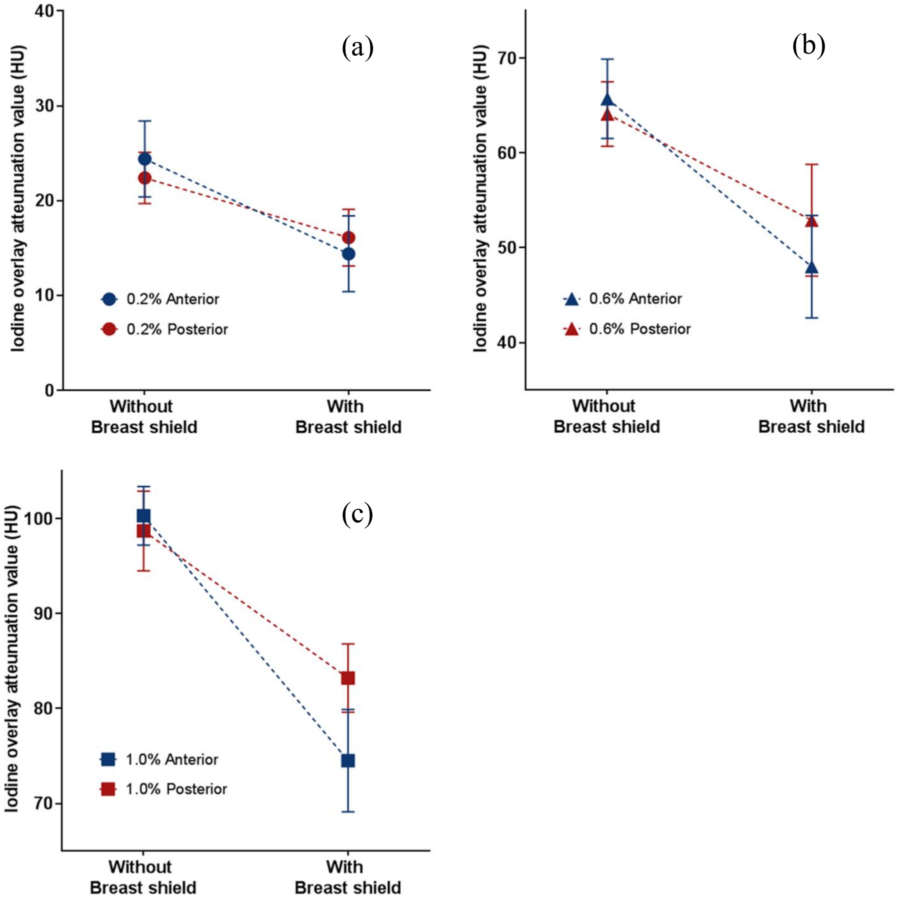

Figure 3. Iodine overlay attenuation values presented as mean values with standard deviations from the nodules at anterior and posterior locations of the dual-energy CT scans with and without bismuth breast shielding for 0.2% (a), 0.6% (b) and 1.0% (c) concentrations.

For the anterior location, the values for the 0.2%, 0.6% and 1.0% nodules found without breast shielding were 24.4 ± 4.0 HU, 65.7 ± 4.2 HU and 100.3 ± 3.1 HU, respectively. After breast shielding, we obtained significantly decreased iodine overlay attenuation values for all three concentrations (P = 0.002 for all) with 14.4 ± 4.0 HU, 48.0 ± 5.4 HU and 74.5 ± 5.4 HU for the 0.2%, 0.6% and 1.0% nodules, respectively.

For the posterior location, we obtained similar results to the anterior location. Iodine overlay attenuation values found without breast shielding were 22.4 ± 2.7 HU, 64.1 ± 3.4 HU and 98.7 ± 4.2 for the 0.2%, 0.6% and 1.0% nodules, respectively. These values were significantly higher compared to DECT scans performed with breast shielding, with values being 16.1 ± 3.0 HU, 52.9 ± 5.9 HU and 83.2 ± 3.6 HU for the 0.2%, 0.6% and 1.0% nodules, respectively (P = 0.002 for all).

In addition, we evaluated the difference in iodine overlay attenuation values according to nodule location. For DECT without breast shielding, there were no significant differences between the anterior and posterior locations for the 0.2%, 0.6% and 1.0% nodules (P = 0.182, 0.272 and 0.308, respectively). After breast shielding, there was no significant difference between the locations for the 0.2% nodules (P = 0.347). However, we obtained significantly decreased iodine overlay attenuation values at the anterior location for the 0.6% and 1.0% nodules (P = 0.007 and 0.002, respectively) compared to the posterior location.

2. Comparison of CT attenuation values on 100-kV and 140-kV CT

CT attenuation values of the 100-kV and 140-kV CT images are summarized in Table 1. For the anterior location, attenuation values of the 0.2%, 0.6% and 1.0% nodules on 100-kV CT with breast shielding were significantly higher than 100-kV CT without breast shielding (P = 0.028, 0.015 and 0.041 respectively). We also observed a significant increase in CT attenuation values for 140-kV CT with breast shielding (P = 0.002 for all).

For the posterior location, there were no significant differences in CT attenuation values for 100-kV CT with breast shielding for the 0.2%, 0.6% and 1.0% nodules (P = 0.158, 0.182 and 0.060). However, for 140-kV CT, CT attenuation values with breast shielding were significantly higher than those without breast shielding for the 0.2%, 0.6% and 1.0% nodules (P = 0.002, 0.006 and 0.005).

CT attenuation values for the 0.2%, 0.6% and 1.0% nodules did not significantly differ between the anterior and posterior locations on 100-kV (P = 0.556, 0.224 and 0.099, respectively) and 140-kV CT (P = 0.388, 0.065 and 0.060, respectively) without breast shielding. However, with the breast shield, significantly higher CT attenuation values were observed at the anterior location than the posterior location in both 100-kV (P = 0.025, 0.002 and 0.002, respectively) and 140-kV CT (P =0.019, 0.002 and 0.002 respectively) for the 0.2%, 0.6% and 1.0% nodules.

Table 1. CT attenuation values of lung nodules on 100-kV and 140-kV CT.

	0.2% Nodule		0.6% Nodule		1.0% Nodule	
	100 kV (HU)	**140 kV (HU)**	**100 kV (HU)**	**140 kV (HU)**	**100 kV (HU)**	**140 kV (HU)**
Anterior						
Without breast shielding	25.7 ± 3.7	15.2 ± 4.0	76.5 ± 4.6	37.1 ± 5.4	120.5 ± 5.0	57.3 ± 4.2
With breast shielding	31.9 ± 7.6	26.2 ± 6.4	82.4 ± 8.4	54.8 ± 9.1	125.7 ± 8.7	77.7 ± 9.7
P value	0.028	0.002	0.015	0.002	0.041	0.002
Posterior						
Without breast shielding	24.2 ± 5.2	17.1 ± 4.5	74.6 ± 4.7	34.4 ± 4.2	114.8 ± 5.7	53.2 ± 6.5
With breast shielding	26.4 ± 2.7	21.5 ± 3.8	72.2 ± 3.1	38.3 ± 4.1	113.0 ± 4.3	57.9 ± 4.9
P value	0.158	0.002	0.182	0.006	0.060	0.005

HU: Hounsfield Unit.

Values are CT numbers (HU) as mean ± standard deviation.

3. Comparison of image noise

The mean value of image noise at the anterior lung on DECT significantly increased after breast shielding (16.18 ± 0.39 HU) compared to the mean value obtained without breast shielding (9.55 ± 0.23 HU) ($P = 0.002$). Likewise, the image noise level at the posterior lung on DECT was significantly higher with breast shielding (14.22 ± 0.65 HU) than without breast shielding (9.81 ± 0.39 HU) ($P = 0.002$). There was no significant difference in the mean value of image noise between the anterior and posterior lungs without breast shielding ($P = 0.082$). However, we observed significantly higher values of image noise at the anterior lung compared to the posterior lung with breast shielding ($P = 0.002$).

4. Comparison of absorbed radiation doses

Absorbed radiation doses are presented in Figure 4. The measured radiation dose of the breast and lung without the breast shield was 4.32 ± 0.33 mGy and 5.53 ± 0.46 mGy, respectively. With the bismuth shield, we observed a significant decrease in radiation dose for both breast (3.68 ± 0.30 mGy) and lung parenchyma (5.29 ± 0.27 mGy). The dose reduction rate was 14.8% for the breast and 4.3% for the lung.

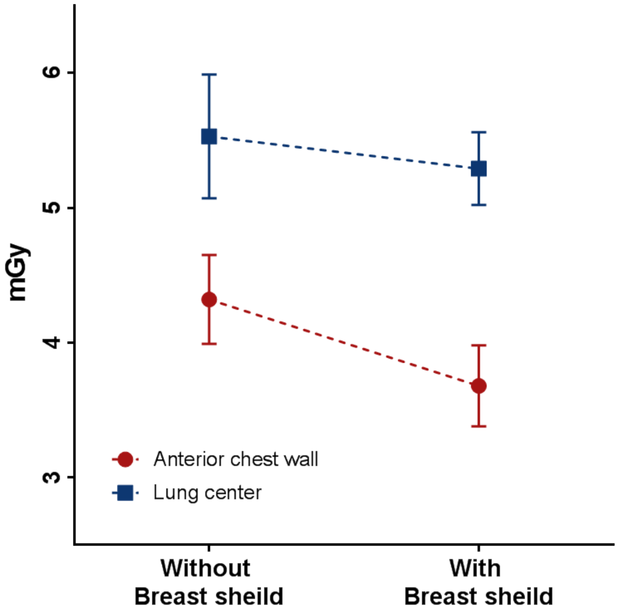

Figure 4. Comparison of absorbed radiation doses between CT scans with and without breast shielding

IV. DISCUSSION

In this study, we evaluated the effects of bismuth breast shielding on iodine differentiation in DECT along with its effect on image noise and radiation dose through a phantom study. The main findings were that applying the bismuth breast shield in DECT not only increases image noise but also significantly decreases iodine overlay attenuation values, although with significantly less radiation exposure to the breast. These findings have not been well established in previous literature.

Although it is clear that the bismuth breast shield can reduce radiation exposure to the breast [13-19], there has been controversy regarding its application during CT scans because of consequent image noise and artifacts. These issues have been discussed in detail with conventional single-energy CT [16,18,22,23]. However, we thought it necessary to evaluate the effects of bismuth breast shielding on DECT because thoracic application of DECT has recently increased with pulmonary functional imaging and thoracic tumor imaging [1,4,21].

In the present study, we observed significant decrease in the iodine overlay attenuation values of nodules after breast shielding, especially at the anterior location. Furthermore, we observed substantially increased CT attenuation values of the nodules, especially at the anterior location and on 140-kV images after breast shielding. A few studies previously reported these increments of CT attenuation with bismuth breast shielding and the increase was thought to be related to metal artifacts from bismuth within the shield

[19,20,24]. Metal materials in the scan field lead to beam hardening, scattering, edge gradient and photon starvation artifacts, which can result in degraded image quality. Because the metal opacity is beyond the range that can be controlled by the computer, an incomplete attenuation profile is ultimately unavoidable. A previous study reported that these findings were noted both near and far from the shield under 120 kV although there was a less pronounced increase in CT attenuation at a farther distance from the shield [20]. Because x-ray beams from the non-shielded portion may contribute more to image reconstruction for the posterior location than beams from the shielded portion, we might observe less prominent but increased CT attenuation at the posterior location [19]. In our study, increased CT attenuation also differed according to distance from the shield with x-ray energy. Increased CT attenuation was observed at the anterior but not the posterior location with 100 kV. For 140 kV, increased CT values were noted at both anterior and posterior locations with less prominence at the posterior location. Iodine can be differentiated and quantitated with the dual-energy technique based on the material decomposition theory. Theoretically, iodine enhancement is presented by a vector of fixed direction but the length depends on iodine attenuation at 100 kV and 140 kV [25]. Therefore, we thought that the increased CT attenuation values after bismuth breast shielding, especially on 140 kV, might affect iodine quantification with significantly decreased iodine overlay attenuation values. Likewise, other material differentiation might be thought to be affected by bismuth shielding based on our study results.

Regarding image noise, we observed significantly increased image noise on the weighted-average 120-kV CT images with the bismuth shield as expected, especially at the anterior location. From our study, we were also to confirm that there was significantly less radiation exposure to the breast with a reduction rate of 14.8% in absorbed radiation dose. However, the reduction rate in our study was relatively lower than the results of previous reports with single-energy CT, which showed values from 29 to 59% for the reduction rate in either effective or absorbed radiation dose [13-19]. One study reported that the radiation dose reduction rate by the bismuth breast shield decreased at higher tube voltage settings [26]. We thought that less radiation dose reduction might be observed in DECT with breast shielding than in single-energy CT because higher tube voltage setting is inevitably used in DECT. However, further studies are needed to reduce radiation exposure with the bismuth breast shield in DECT.

There are some limitations in our study. First, we used balloons to mimic lung nodules for this study which were prepared with mixtures of water and iodine, and these balloons have different compositions than true lung nodules with various soft components. Nevertheless, we thought that the effects of breast shielding on iodine differentiation and quantification in DECT might be difficult to evaluate in humans due to the different contrast enhancement times between CT scans performed with and without breast shielding and radiation dose issues. Second, we evaluated the effect of bismuth breast shield with a signle phantom size. According to previous study and the result of our study, the shift of CT attenuation number is affected by the distance from the breast shield [20]. Different sizes of patient may affect the measurement of dual energy CT, and further investigation with different phantom size could be followed. Third, because the phantom did not simulate the developed breast, we measured radiation doses at the surface of the anterior chest wall. The measured radiation doses in this study might not be identical to results found at the mid-portion of the simulated or true breast. Finally, we used dual x-ray sources in DECT, which could cause cross-scattered radiation. Also, we used 100-kV and 140-kV settings in the present study. Further studies might be needed with other dual-energy techniques such as rapid tube potential switching or multilayer detectors and different kV settings.

V. CONCLUSION

In conclusion, although the bismuth breast shield can decrease radiation exposure to the breast during DECT, it significantly affects iodine quantification with decreasing iodine overlay attenuation values along with an increase in image noise. Breast shielding might also affect other material differentiation. Therefore, the bismuth breast shield should not be used in DECT. Instead, we recommend radiologists to consider alternative methods, such as globally decreasing tube current without breast shield, to reduce radiation exposure to the breast. Further studies are needed on bismuth breast shielding in DECT.

연세대학교
YONSEI UNIVERSITY

REFERENCES

1. Kang M-J, Park CM, Lee C-H, Goo JM, Lee HJ. Dual-Energy CT: Clinical Applications in Various Pulmonary Diseases 1. Radiographics 2010;30:685-98.
2. Johnson T, Fink C, Sch nberg SO, Reiser MF. Dual energy CT in clinical practice: Springer Science & Business Media; 2011.
3. Johnson TR. Dual-energy CT: general principles. American Journal of Roentgenology 2012;199:S3-S8.
4. Ko JP, Brandman S, Stember J, Naidich DP. Dual-energy computed tomography: concepts, performance, and thoracic applications. Journal of thoracic imaging 2012;27:7-22.
5. Di Chiro G, Brooks RA, Kessler RM, Johnston GS, Jones AE, Herdt JR, et al. Tissue Signatures with Dual-Energy Computed Tomography 1. Radiology 1979;131:521-3.
6. GENANT HK, Boyd D. Quantitative bone mineral analysis using dual energy computed tomography. Investigative radiology 1977;12:545-51.
7. Millner MR, McDavid WD, Waggener RG, Dennis MJ, Payne WH, Sank VJ. Extraction of information from CT scans at different energies. Medical physics 1979;6:70-1.
8. Li B, Yadava G, Hsieh J, Chandra N, Kulpins MS. Head and body CTDIw of dual-energy x-ray CT with fast-kVp switching. SPIE Medical Imaging: International Society for Optics and Photonics; 2010. p.76221Y-Y-12.
9. Ho LM, Yoshizumi TT, Hurwitz LM, Nelson RC, Marin D, Toncheva G, et al. Dual energy versus single energy MDCT: measurement of radiation dose using adult abdominal imaging protocols. Academic radiology 2009;16:1400-7.
10. Samet JM. Epidemiologic studies of ionizing radiation and cancer: past successes and future challenges. Environmental health perspectives 1997;105:883.

11. Gilbert ES. Ionising radiation and cancer risks: what have we learned from epidemiology? International journal of radiation biology 2009;85:467-82.
12. Radiation UNSCotEoA. Sources and effects of ionizing radiation (UNSCEAR 2008). Annex D: Health effects due to radiation from the Chernobyl accident. New York: United Nations 2011.
13. Fricke BL, Donnelly LF, Frush DP, Yoshizumi T, Varchena V, Poe SA, et al. In-plane bismuth breast shields for pediatric CT: effects on radiation dose and image quality using experimental and clinical data. American Journal of Roentgenology 2003;180:407-11.
14. Hopper KD. Orbital, thyroid, and breast superficial radiation shielding for patients undergoing diagnostic CT. Seminars in Ultrasound, CT and MRI: Elsevier; 2002. p.423-7.
15. Hopper KD, King SH, Lobell M, TenHave T, Weaver J. The breast: in-plane x-ray protection during diagnostic thoracic CT--shielding with bismuth radioprotective garments. Radiology 1997;205:853-8.
16. Wang J, Duan X, Christner JA, Leng S, Yu L, McCollough CH. Radiation dose reduction to the breast in thoracic CT: comparison of bismuth shielding, organ-based tube current modulation, and use of a globally decreased tube current. Medical physics 2011;38:6084-92.
17. Geleijns J, Artells MS, Veldkamp W, Tortosa ML, Cantera AC. Quantitative assessment of selective in-plane shielding of tissues in computed tomography through evaluation of absorbed dose and image quality. European radiology 2006;16:2334-40.
18. Vollmar SV, Kalender WA. Reduction of dose to the female breast in thoracic CT: a comparison of standard-protocol, bismuth-shielded, partial and tube-current-modulated CT examinations. European radiology 2008;18:1674-82.
19. Kalra MK, Dang P, Singh S, Saini S, Shepard J-AO. In-plane shielding for CT: effect of off-centering, automatic exposure control and shield-to-surface distance. Korean Journal of Radiology

2009;10:156-63.

20. Goldin D, Emerson S, Farah MC, Sokhandon F, Nandalur KR, Kumar S, et al. Shielding artificially increases the attenuation of water: study of CT gradient attenuation induced by shielding (CT GAINS). Academic radiology 2013;20:231-7.

21. Remy-Jardin M, Faivre J-B, Pontana F, Molinari F, Tacelli N, Remy J. Thoracic applications of dual energy. Seminars in respiratory and critical care medicine; 2014. p.64-73.

22. McCollough CH, Wang J, Berland LL. Bismuth shields for CT dose reduction: do they help or hurt? Journal of the American College of Radiology 2011;8:878-9.

23. Colletti PM, Micheli OA, Lee KH. To shield or not to shield: application of bismuth breast shields. American Journal of Roentgenology 2013;200:503-7.

24. Lee YH, Park E-t, Cho PK, Seo HS, Je B-K, Suh S-i, et al. Comparative analysis of radiation dose and image quality between thyroid shielding and unshielding during CT examination of the neck. American Journal of Roentgenology 2011;196:611-5.

25. Kalender WA, Klotz E, Kostaridou L. An algorithm for noise suppression in dual energy CT material density images. Medical Imaging, IEEE Transactions on 1988;7:218-24.

26. Seoung Y-H. Evaluation of radiation dose reduction during CT scans by using bismuth oxide and nano-barium sulfate shields. Journal of the Korean Physical Society 2015;67:1-6.

ABSTRACT(IN KOREAN)

흉부모형 실험을 통한 이중에너지 전산화단층촬영에서 비스무트 유방차폐제가 검사에 미치는 영향 분석

<지도교수 이 혜 정>

연세대학교 대학원 의학과

장 현 식

목적: 이중에너지 전산화단층촬영에서 비스무트 유방차폐제가 요오드 정량화와 방사선 조사량에 미치는 영향을 흉부모형을 이용하여 분석한다.

대상 및 방법: 물과 이오파미돌(iopamidol) 조영제를 각각 0.2%, 0.6% 및 1.0%농도로 섞어 작은 고무풍선을 채워 세 개의 각기 다른 요오드농도의 폐 결절을 재현하였다. 고무풍선들을 흉부모형의 폐 앞쪽과 뒤쪽에 위치시킨 후 이중에너지 전산화 단층촬영을 시행하였다. 각각의 농도의 고무풍선들에 대해 유방 차폐제를 사용하지 않고 영상을

촬영한 후 유방차폐를 사용하고 다시 영상을 촬영하였다. 이후 얻어진 요오드 영상에서, 각각의 폐 결절에 대해 원형 관심영역을 설정하여 요오드의 오버레이(overlay) 감쇄계수를 측정하였다. 또한 선량계를 이용하여 유방의 방사선 흡수선량을 측정하였다. 세 농도의 결절에 대해서 각각 유방차폐를 사용하기 전후 12쌍의 요오드 오버레이 감쇄계수를 측정하였다. 측정된 결과값들은 윌콕슨 부호 순위 테스트를 이용하여 분석하였다.

결과: 유방차폐를 시행한 경우, 폐의 앞쪽에 배치시킨 결절은 0.2%, 0.6%, 1.0% 농도 모두에서 요오드 오버레이 감쇠계수가 감소하였다 (P = 0.002). 폐의 뒤쪽에 배치시킨 결절 역시 유방차폐를 시행한 경우 세 농도 모두에서 요오드 오버레이 감쇄계수가 감소하였다 (P = 0.002). 유방차폐를 시행한 경우 유방의 방사선 흡수선량은 14.8%감소하는 결과를 보였다 (P = 0.005).

결론: 유방차폐를 사용함으로써 유방의 방사선 노출을 줄일 수 있지만 이중 에너지 전산화 단층 촬영 검사에서 이는 요오드 정량화 분석에 영향을 미칠 수 있다.

핵심되는 말: 비스무트 유방차폐, 방사선 흡수선량, 이중에너지 전산화 단층 촬영, 요오드 정량화 분석